Characterization of the current-induced resistive spots in superconducting $$\hbox {YBa}_{2} \hbox {Cu}_{3} \hbox {O}_{7}$$ YBa 2 Cu 3 O 7 strips

K. Harrabi, A. F. Salem, K. Ziq, A. I. Mansour, S. Kunwar, J. P. Maneval & G. Berdiyorov

Applied Physics A
Materials Science & Processing

ISSN 0947-8396
Volume 117
Number 4

Appl. Phys. A (2014) 117:2033-2036
DOI 10.1007/s00339-014-8613-y

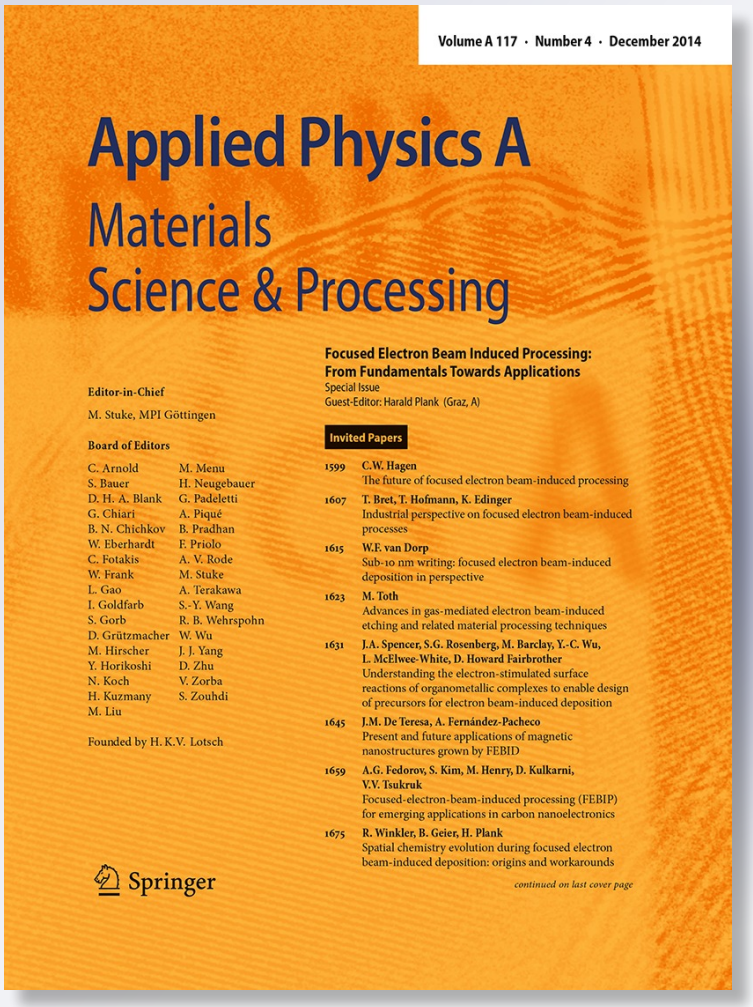

Springer

Appl. Phys. A (2014) 117:2033–2036
DOI 10.1007/s00339-014-8613-y

Applied Physics A
Materials Science & Processing

Characterization of the current-induced resistive spots in superconducting $YBa_2Cu_3O_7$ strips

K. Harrabi · A. F. Salem · K. Ziq · A. I. Mansour · S. Kunwar · J. P. Maneval · G. Berdiyorov

Received: 27 January 2014 / Accepted: 10 July 2014 / Published online: 6 August 2014

Abstract For over a decade, ultrathin superconducting films have been developed for the detection of single photons at optical or near infrared frequencies, with competitive performances in terms of quantum efficiency, speed, and low dark count rate. In order to avoid the requirement of helium refrigeration, we consider here the use of high temperature materials, known to achieve very fast responsiveness to laser irradiation. We excite thin filaments of the cuprate $YBa_2Cu_3O_7$ by rectangular pulses of supercritical current so as to produce either a phase-slip centre (PSC) or a normal hot spot (HS), according to the temperature and the current amplitude selected. That procedure provides information about the maximum bias current to be used in a particle detector, about the return current back to the quiescent state after excitation, and about the rate of growth and decay of a HS. We also measure the time of PSC nucleation. A unique feature of that approach is to provide the rate of heat transfer between the film and its substrate at whatever temperature, in the superconducting state, in the practical conditions of operation.

1 Introduction

Single-photon detectors based on Superconducting Nanowires (SNSPDs) have been developed recently [1], with competitive performances in terms of quantum efficiency, speed, and dark count rates. The materials selected so far have been mainly the ultrathin ($\sim$5 nm) strips made of sputtered NbN [1, 2], $Nb_xTi_{1-x}N$ [3], or Nb [4], which have an adequate lasting time and a critical transition temperature T_c in a convenient range above the liquid helium temperature. In addition, since the first reports of single photon detection in NbN films, these devices have proved efficient in the detection of other single particles such as molecular ions or molecules [5], or keV electrons from a scanning electron microscope (SEM) microscope [6].

However, in order to avoid the requirement of helium refrigeration, and in view of the very high speed of response of the high-T_c material $YBa_2Cu_3O_7$ (YBCO for brief) in the hot-electron mode [7, 8], we consider here YBCO thin films as possible substitutes for low-T_c materials. Our experimental method, which involves the voltage response to nanosecond electrical pulses, provides data on the film thermal parameters not only in the bolometric sensitivity range around T_c, but also far below T_c, in the zero-resistance state prior to a detection event. The resistive states expected for quasi 1-D transport, namely phase-slip centres (PSC) [10] and localized hot spots (HS) [11], have also been observed in YBCO strips [9]. The current-controlled drive discriminates stable-in-time phase-slip centre structures near T_c from expanding HS at lower temperatures. The voltage that appears after a delay time t_d readily distinguishes a PSC signal from other types of resistive response, such as the presumably instantaneous vortex flow (VF) response [12, 13].

2 Sample and experimental setup

The YBCO thin films, purchased from Theva GmbH (Germany), were grown by thermal co-evaporation. The R-

K. Harrabi (✉) · A. F. Salem · K. Ziq · A. I. Mansour · S. Kunwar · G. Berdiyorov
Physics Department, King Fahd University of Petroleum and Minerals, 31261 Dhahran, Saudi Arabia
e-mail: harrabi@kfupm.edu.sa

J. P. Maneval
Laboratoire Pierre Aigrain, ENS 24 rue Lhomond, Paris 75231, France

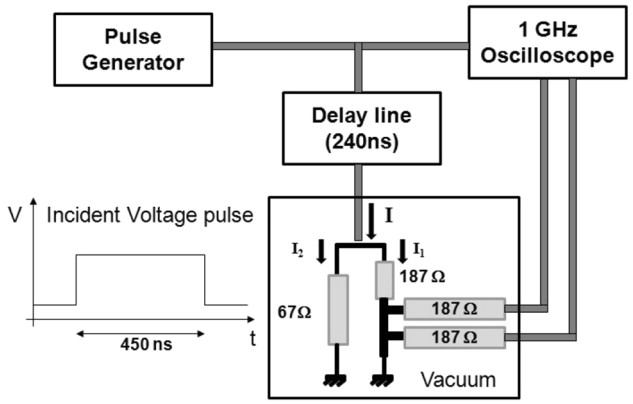

Fig. 1 Sketch of the experimental setup used for pulse measurements. It consists of a step generator, a delay line to separate the incident pulse from the reflected one, and an oscilloscope is used to measure the voltage through lateral probes and the delay time t_d. The variable-temperature part is enclosed in a rectangle

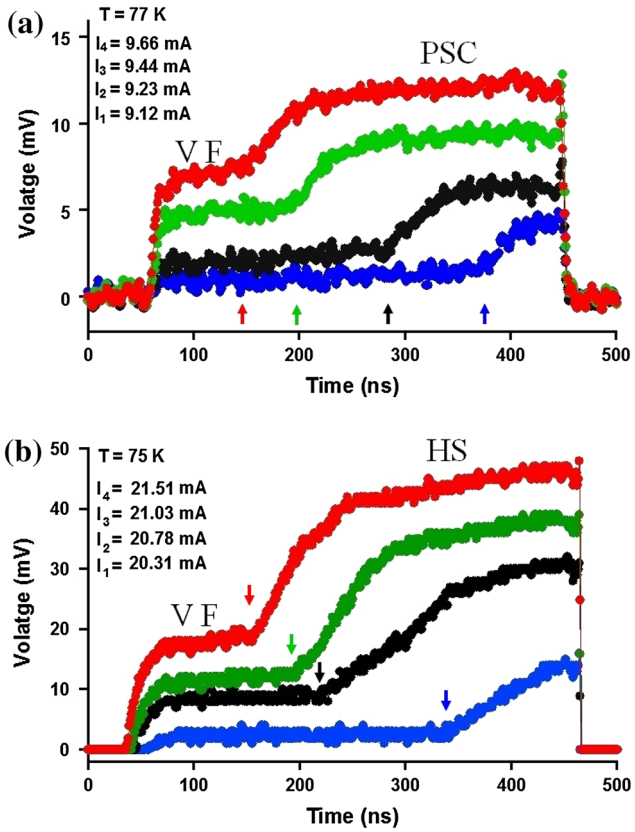

Fig. 2 **a** Voltage response to a rectangular current pulse versus time at $T = 77$ K and for different current values. The increase in voltage before the nucleation of PSC corresponds to flux flow. **b** Voltage versus time, showing the transformation of PSC to HS at $T = 75$ K, where the voltage is rising with time compared with the ones in **a**

cut sapphire substrates were coated with a 40-nm epitaxial cerium oxide buffer layer prior to deposition of the YBCO with film thickness $b = 80$ nm. On top of the YBCO film, a 100-nm gold layer was applied in situ to cover the contact pads. Afterwards, the devices were patterned to a width $w = 5$ μm using standard photo-lithography processes and ion milling.

The measurement was performed in 15-K closed-cycle cryofree refrigerator with temperature controller. From the resistance versus temperature measured using a DC current source, the transition temperature and the resistivity at 100 K were found to be $T_c = 84\,\mathrm{K}$ and $\rho(100\,K) = 108\,\mu\Omega$ cm. For the pulse measurements, electrical pulses of 450 ns duration at a repetition rate of 10 kHz were sent to the sample through coaxial cables of wave impedance $Z = 50\ \Omega$. In order to maintain a constant bias current through the sample, a 187 Ω resistor was mounted in series with the filament. For better match with the coaxial line impedance, a 67 Ω resistor was placed in shunt on that structure. The equivalent impedance at the line's terminal being 50 Ω in the superconducting state, the reflected signal is eliminated [12]. In this configuration, assuming lossless coaxial cables and negligible contact resistances, the current through the strip I_1 is $\sim 0.264\ V_i/Z$, where V_i is the incident voltage.

The voltage responses were taken from lateral probes in series with 187 Ω resistors to avoid subtracting current from the main line. The system is schematically represented in Fig. 1.

3 Determination of the cooling time of the YBCO film

We used a step-pulse of current as an excitation to discriminate between the different dissipative modes in thin film superconductors. Close to T_c, vortices are always present in YBCO, and become mobile beyond a certain "depinning" current. The dissipation is then distributed uniformly across the whole strip. However, at lower temperatures starting at about 0.9 T_c, the vortex resistance is reduced, making it possible to reach the second, or pair-breaking, critical current $I_c(T)$, above which localized resistive structures, PSCs and HSs, are nucleated. From the voltage response, we can distinguish between the three dissipative modes VF, PSC and HS. The PSC is discriminated from vortex flow by a delay time t_d. The first plateau voltage appearing in each of the Fig. 2a, b is due to vortex flow. Then the increase in voltage shows the appearance of a localized resistive centre (at instants marked by the vertical arrows). In addition, a PSC is also distinguished from a hotspot in the voltage response. Both modes present a voltage after a delay time t_d. A saturating voltage is interpreted as a PSC (Fig. 2a). A voltage that keeps rising is identified as an expanding HS (Fig. 2b).

The delay time t_d described by a time-dependent Ginzburg-Landau (TDGL) equation simplified to the zero-dimensional case is given by [14]:

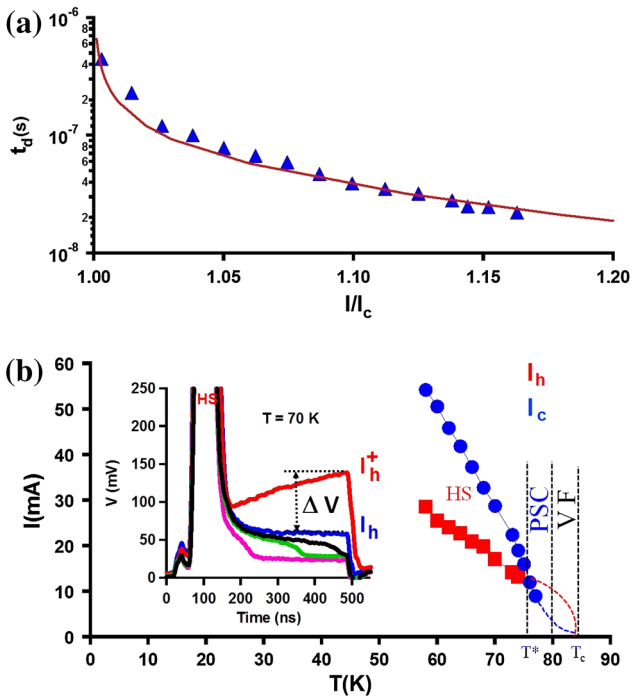

Fig. 3 **a** Delay time t_d versus ratio of the applied current to the critical current I_c. The *red curve* is the Tinkham's fitting function for $T/T_c = 0.9$ with the prefactor $\tau_d = 6$ ns. **b** Temperature dependence of the pair-breaking current I_c and the HS current I_h. The *inset* shows the voltage responses to the superposed current pulses used to determine the hot spot current I_h at $T < T^*$. A large current value initiates the HS and the plateau pulse maintains a stable HS. The HS current I_h in the frontier current between I_h^+ and the lower current that produces a HS in regression (*blue color*)

$$t_d(I/I_c) = \tau_d \int_0^1 \frac{2f^4 \mathrm{df}}{\frac{4}{27}\left(\frac{I}{I_c}\right)^2 - f^4 + f^6} \tag{1}$$

where the pre-factor τ_d of the integral was interpreted as the gap relaxation time, in close connection with the electron–phonon relaxation time τ_{ep}. In the more accurate analysis of Tinkham [15], the pre-factor τ_d has the same meaning, but the integral becomes a function of the two parameters T/T_c and I/I_c. The model was successfully applied to t_d-measurements in indium [16], leading to the result $\tau_{ep}(T_c) = 0.148$ ns, in agreement with other determinations of that quantity in indium. In the case of YBCO strips, the measured t_d's [9, 17] could be accounted for by the Tinkham analysis, with an important difference on the interpretation of the pre-factor τ_d though. It was found to be essentially temperature-independent, proportional to the film thickness [9], and therefore interpreted as a film cooling time, only slightly different from the phonon escape time τ_{esc}. For the combination YBCO on MgO, the result $\tau_{esc}/\mathrm{ps} = 75$ (b/nm) was found. By applying the same Tinkham analysis to the present data (Fig. 3a), one finds at $T = 0.9\ T_c$ an agreement for the choice $\tau_d = 6$ ns (Fig. 3a).

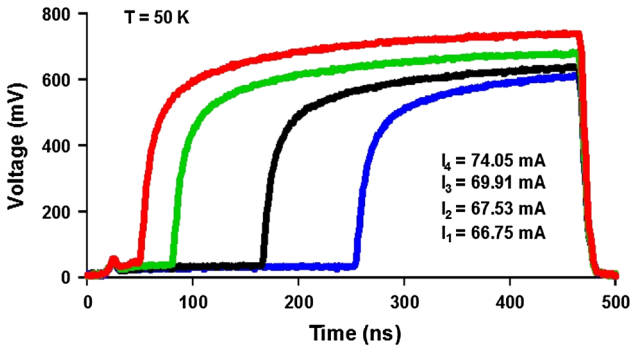

Fig. 4 Voltage response to a current versus time at 50 K < T^*, and for different current values. The sudden increase in voltage is due to the nucleation of a PSC immediately transformed into a HS. The quasi-saturation of the voltage is caused by current drop due to the high HS resistance

In consideration of the thickness ($b = 80$ nm), this gives the same ratio τ_{esc}/b as before, although the substrate is now sapphire instead of MgO. Let us remember that the reset time of a thin-film superconducting detector is determined by two independent components: (1) an electronic one due to the kinetic inductance [18], and (2) a purely thermal relaxation process. The latter is expressed by the cooling time $\simeq$ phonon escape time.

In Fig. 2a, at $T = 77$ K, the PSC voltage can be obtained by subtracting the VF plateau that is visible at short times from the total voltage observed on the long-term after t_d. This V_{PSC} turns out to vary linearly with the applied current, according to the relation $V_{PSC} = R_u(I - I_s)$. Here, $R_u = \partial V_{PSC}/\partial I = 2.5\,\Omega$ is the differential resistance and I_s, the excess superconducting current, equals 5.7 mA, to be compared with 1/2 $I_c = 4.5$ mA. The slope R_u gives access to the quasi-particle diffusion length [10] through $R_u = 2\rho\Lambda/wb$, with the result $\Lambda = 0.46\,\mu$m. As a consequence, the PSC appears as an ohmic spot of length $L = 2\ \Lambda = 0.92\ \mu$m. The τ_d, experimentally determined, is an effective cooling time, and allows for the defining of an effective PSC temperature by:

$$\frac{\rho I(I - I_s)}{(w \cdot b)^2} = \frac{\int C\mathrm{dT}}{\tau_d \cdot (w \cdot b)} = \frac{H(T_{PSC}) - H(T)}{\tau_d} \tag{2}$$

where C is the volumetric specific heat of YBCO [19], the integral extends from T to T_{PSC}, and H is the enthalpy of YBCO per unit volume. For trace 3 of Fig. 2a, with $I = 9.44$ mA, we find $T_{PSC} = 82$ K, coming close, but still inferior to $T_c = 84$ K.

We now consider the low temperature domain (typically $T = 70$ K), where the vortex flow is frozen. In this case, to measure I_h, we used two superposed current pulses. The first pulse is sent to initiate the HS and the second one to maintain its stability (inset of Fig. 3b). We observe a variety of behaviours depending upon the current

amplitude. For current $I = I_h^+$, the rising voltage indicates a growing HS (upper red trace). For $I = I_h$, the constant voltage corresponds to the minimum current able to sustain a stable HS. For a lower current, there is either a slowly descending voltage (HS in regression), or a rapid fall to zero (lower magenta trace). The limit between the two last behaviours is supposed to be the current able to maintain the temperature T_c in an unlimited strip. The expanding velocity of the hot spot can be determined from the linear increase of the voltage *versus* time in Fig. 3b, and is given by:

$$U = \frac{w \cdot b}{2I \cdot \rho_{100\,K}} \cdot \frac{\mathrm{dV}}{\mathrm{d}t} = 3.2\,\mathrm{m/s}. \quad (3)$$

The voltage responses of Fig. 4, taken at $T = 50$ K, illustrate the limitations, but also the superiorities of the pulse method. On the one hand, they very clearly show the dependence of the delay time upon the current amplitude, from which the phonon escape time is derived, since $T < T^*$, $I_c > I_h$ and the PSC just formed at t_d immediately turns into a growing hot spot [13]. From the specifications of the circuit (Fig. 1), the current amplitude at $t = 0$ (trace 1 ; $I = 66.75$ mA), and the saturated voltage, estimated at ~ 600 mV, one deduces $R_{HS} \sim 20\,\Omega$. By using the relation $R = \rho L_n/(w \cdot b)$, we get the HS length $L_n \sim 7.35$ µm. Due to the negative feedback of the HS voltage drop, the current itself has fallen by 40 % of its initial value. To emphasize the likeliness of these considerations, we evaluate the temperature TM at the HS centre by using the relation $\rho I^2/w^2 \cdot b^2 = C(T_{HS} - T)/\tau_{esc}$ with a specific heat $C \sim 1$ J cm^{-3} K^{-1}. One finds $T_{HS} \sim 115$ K, not far from the temperature symmetrical of T with respect to T_c, which is the usual prescription in a linear model of heat transfer [11].

4 A possible use of YBCO for single particle detection

The very high responsivity and speed of YBCO thin film detectors [7, 8, 20] was attributed to their hot electron response. However, in view of their specific heat $C_{YBCO}(77K) \sim 1$ J K^{-1} cm^{-3} compared to the low-T_c $C_{Nb}(5K) \sim 0.005$ J K^{-1} cm^{-3}, the detection of single optical photon is ruled out. That conclusion does not apply to more energetic single particles, provided that their possible deteriorating effects can be avoided. YBCO thin film working at 77 K would then provide a sharp timing of the detection event, and an intrinsic thermal reset time of the same order—for equal thickness—as the low T_c thin film device.

5 Conclusion

Narrow c-axis–oriented YBCO strips (on sapphire substrate) submitted to an overcritical current behave similarly to low T_c materials. The dissipation occurs in localized spots of two types: phase slip centres and normal hot spots, whose threshold currents $I_c(T)$ and $I_h(T)$ were measured by using pulse techniques. The times of nucleation of PSCs, analyzed according to the TDGL theory allowed us to derive a heat escape time of 6 nanoseconds for 80 nm of thickness, or 75 ps per nm, a result already obtained for YBCO films directly deposited on MgO crystals.

Acknowledgments The authors gratefully acknowledge the support of the King Fahd University of Petroleum and Minerals, Saudi Arabia, for funding this research (DSR-IN100034).

References

1. G.N. Gol'tsman et al., App. Phys. Lett. **79**, 705 (2001)
2. A. Semenov, G.N. Goltsman, A.A. Korneev, Physica C **351**, 349 (2001)
3. S.N. Dorenbos, E.M. Reiger, U. Perinetti, V. Zwiller, T. Zijlstra, T.M. Klapwijk, Appl. Phys. Lett. **93**, 131101 (2008)
4. A.J. Annunziata et al., IEEE Trans. Appl. Supercond. **19**, 327 (2009)
5. N. Zen et al., App. Phys. Lett. **95**, 172508 (2009)
6. M. Rosticher et al., Appl. Phys. Lett. **97**, 1 (2010)
7. A. Ghis, S. Pfister, J.-C. Villégier, M. Nail, J.-P. Maneval, IEEE Trans. Appl. Supercond. **3**, 2136 (1993)
8. P. Thoma et al., IEEE Trans. Appl. Supercond. **3**, 2400206 (2013)
9. K. Harrabi, F.R. Ladan, Vu Dinh Lam, J.-P. Maneval, J.-F. Hamet, J.-P. Villégier, R.W. Bland, J. Low Temp. Phys. **157**, 36 (2009)
10. W.J. Skocpol, M.R. Beasley, M. Tinkham, J. Low Temp. Phys. **16**, 145 (1974)
11. W.J. Skocpol, M.R. Beasley, M. Tinkham, J. Appl. Phys. **45**, 4054 (1974)
12. K. Harrabi, J. Supercond. Nov. Magn. **26**, 1865 (2013)
13. F.-R. Ladan, Kh Harrabi, M. Rosticher, C. Villard, P. Mathieu, J.-P. Maneval, J. Low Temp. Phys. **153**, 103 (2008)
14. J.A. Pals, J. Wolter, Phys. Lett. A **70**, 150 (1979)
15. M. Tinkham, in *Nonequilibrium, Superconductiviitvyi, Phonons, and Kapitza Boundaries, Proceedings of NATO Advanced Study Institutes B 65*, ed. by K.E. Gray (Plenum, New York, 1981), p. 231
16. D.J. Frank, M. Tinkham, Phys. Rev. B **28**, 5345 (1983)
17. F.S. Jelila, J.P. Maneval, F.R. Ladan, F. Chibane, A. Marie-de-Ficquelmont, L. Mchin, J.-C. Villégier, M. Aprili, J. Lesueur, Phys. Rev. Lett. **81**, 1933 (1998)
18. C.M. Natarajan, M.G. Tanner, R.H. Hadfield, Supercond. Sci. Technol. **25**, 063001 (2012)
19. M. Onuki, T. Fujiyoshi, H. Ohsumi, H. Kubota, T. Hoshino, Physica C **235–240**, 1383 (1994)
20. B.S. Karasik, M.A. Zorin, I.I. Milostnaya, A.I. Elantev, G.N. Gol'tsman, E.M. Gershenzon, J. App. Phys. **77**, 4064 (1995)